Progress in Materials Chemistry and Physics (2022)
Clausius Scientific Press, Canada

DOI: 10.23977/pmcp.2022.030101
ISSN 2616-3780 Vol. 3 Num. 1

Microstructural and Mössbauer Studies of Samarium Doped $Cu_{0.5}Co_{0.5}Fe_{2-x}Sm_xO_4$ Nanoferrites

Kaimin Su[1], Guangbai Yuan[1], Hu Yang[1,*], Yun He[2,*]

[1]College of Physics and Technology, Guangxi Normal University, Guilin 541004, China.
[2]Guangxi Key Laboratory of Nuclear Physics and Nuclear Technology, Guangxi Normal University, Guilin 541004, China.
**corresponding author*

Keywords: Cu-Co Ferrite, Sol-gel method, Structure, Mössbauer, Magnetic.

Abstract: Samarium substituted cobalt ferrite $Cu_{0.5}Co_{0.5}Fe_{2-x}Sm_xO_4$ (x=0~0.05) powders have been prepared by a sol-gel auto-combustion method. XRD results indicate that the production of a single cubic phase of ferrites. The lattice parameter decrease and the average crystallite size also decrease with the substitution Sm^{3+} ions. SEM shows that the ferrite powers are nanoparticles. Room temperature Mössbauer spectra of $Cu_{0.5}Co_{0.5}Fe_{2-x}Sm_xO_4$ is two normal Zeeman-split sextets, which display ferrimagnetic behavior. The saturation magnetization and residual magnetization all decrease with the incorporation of the Sm^{3+}. But the coercivity shows no significant change when the content $x \leq 0.03$, but the coercivity abruptly increase up to 1128.9 Oe when x=0.05 with the Sm^{3+} ions doping.

1. Introduction

Ferrite, which derived from iron oxides, has attracted great attention due to their special properties in fundamental physicsand potential technological application[1]. Copper ferrite is one of the very important magnetic material[2-3]. Because it also has the properties of magnetic, magneto-optical, semiconductiong, high thermal stability and electronic conductivity. It can be used for magnetic recording media, anode materials and biomagnetic and biomedicine materials[4-5]. In our work, the series samples of $Cu_{0.5}Co_{0.5}Fe_{2-x}Sm_xO_4$ ($0.0 \leq x \leq 0.05$) powders were prepared by the sol-gel method. Our aim of this study is to research the varication structural and magnetic properties of Cu-Co ferrite by replacement small amounts of samarium.

2. Experiment Section and Synthesis

Rare earth ions substituted cobalt ferrite $Cu_{0.5}Co_{0.5}Fe_{2-x}Sm_xO_4$ (x=0~0.05) powders were prepared by a sol-gel auto-combustion method. The XRD, SEM, MPMS and Mössbauer spectrometer were used to investigate the microstructure and magnetic properties of $Cu_{0.5}Co_{0.5}Fe_{2-x}Sm_xO_4$.

3. Results and Discussion

3.1. XRD Patterns and Structures Analysis

Figure 1 shows the XRD pattern of $Cu_{0.5}Co_{0.5}Fe_{2-x}Sm_xO_4$($x$=0~0.05) ferrites calcined at 900 ℃ for 3h, all diffraction peaks can be indexed to the cubic spinel structure of $CuFe_2O_4$(JCPDS card no.34-0425). The impurity peak is not discovered obviously in these samples. The small map (311) peaks of Figure 1 is an enlarged view of each samples. It indicates that all diffraction peaks widen and diffraction peaks move to the direction of the large diffraction angle with increasing amounts of samarium. This is a characteristic of nanocrystals ferrites and illustrating the lattice parameters decrease with the increasing content of samarium. There is a little impurity peak of $SmFeO_3$ appears in the XRD pattern when x=0.05. Because there are a lot of cacancies in the spinel crystal structure, the metals occupy only a small amount of sublattice sites. When calcined samples, the samarium not only replaced of part iron to form spinel ferrite but also entered the vacancies to form $SmFeO_3$.

Lattice constant and the grain size of the sample is calculated by Scherrer formular[6, 7]:

$$D = k\lambda / h\cos\theta \tag{1}$$

The D represents the particle radius, k is the shape factor of particle, h and θ are the full width at half maximum and the diffraction angle of the correlation peaks. Crystal parameters obtained by calculation with the doping concentration are shown in Figure 2.

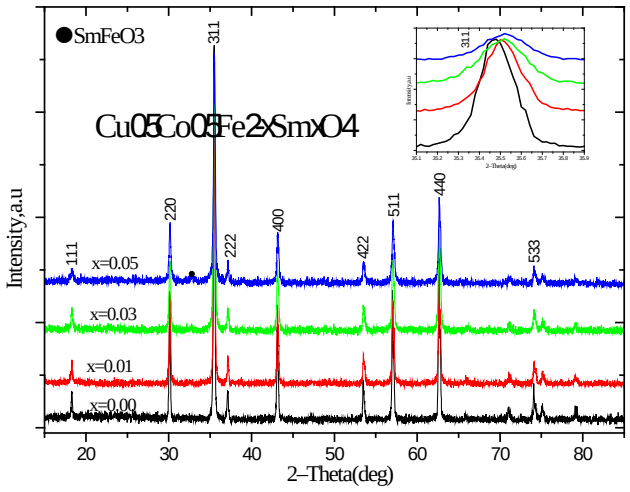

Figure 1: X-ray diffraction patterns of Cu0.5Co0.5Fe2-xSmxO4 calcined at 900 ℃ for 3h.

It shows that the lattice parameter and average crystallite size of samples decrease with increasing doping concentration of Sm content. Although the lattice constant decreases, but the change is not significant. The average crystallite size of samples decrease obviously from 65nm to 38nm. After doping samarium, it causes lattice distortion and increases energy of crystallization, hindering the growth of grains. In addition, the energy of bonding of Sm^{3+}-O^{2-} is higher than Fe^{3+}-O^{2-}. Therefore, it causes the crystal need to absorb more heat to formatting crystallization. The two reasons will refine the particle of samples[7-8].

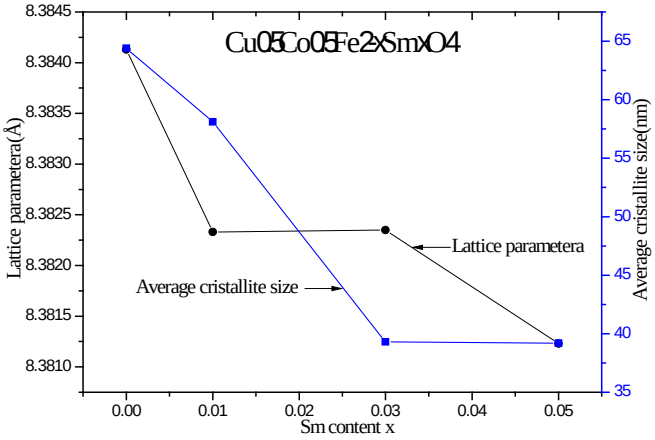

Figure 2: The variation of lattice parameter and average crystallite size with the Sm content.

3.2. Structures and grain size

There are two dimension of SEM micrographs show in Fig.3 when x=0, 0.01. The crystalline samples of $Cu_{0.5}Co_{0.5}Fe_2O_4$ are better, larger particles and grain boundaries significantly. However, there is a wide distribution of particle size. The crystalline samples are still well and the grain boundaries are still significant. But the size of particles are smaller and the distribution of particle size are narrow. All exterior shape of the particles are almost spherical. Moreover, on the basis of characteristic of SEM image formation: the brightness of the SEM image is proportional to the productivity of secondary electrons. At the same time, the productivity of secondary electrons are major depend on the situation of samples surface. Convex surface of the particles, the more secondary electrons generated. the shape of the concave surface of the particles, the less the secondary electrons produced. By contrast, unincorporated photos brighter than incorporation. It explains that the particles of $Cu_{0.5}Co_{0.5}Fe_{1.99}Sm_{0.01}O_4$ have more cracks than the particles of $Cu_{0.5}Co_{0.5}Fe_2O_4$.

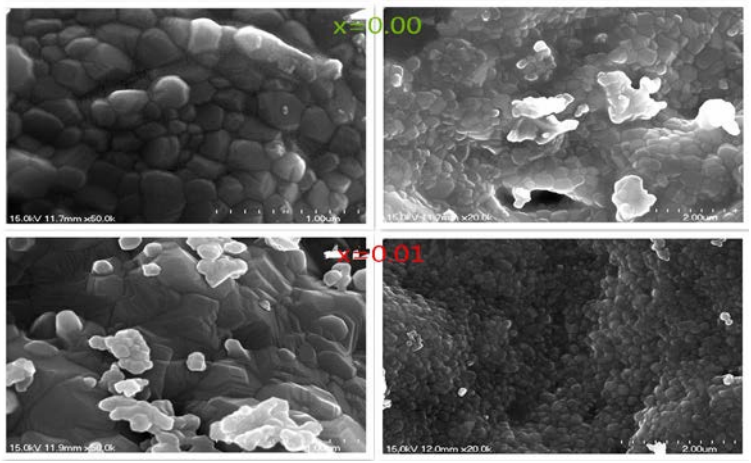

Figure 3: SEM micrographs of Cu0.5Co0.5Fe2-xSmxO4 (x=0, 0.01) ferrites calcined at 900 ℃.

3.3. Mössbauer Spectroscopy Anaysis

The Mössbauer spectra recorded at room temperature are shown in Fig.4 for $Cu_{0.5}Co_{0.5}Fe_{2-x}Sm_xO_4$ (x=0~0.05). All samples have been analysed using Mösswinn 3.0 programme. It is reported that the values of I.S. for Fe^{2+} ions lie in the range 0.6~1.7 mm/s, while for Fe^{3+} ions they lie in the range 0.1~0.5 mm/s[9, 10]. From the Table 1, we get the values for I.S. in the range 0.211~0.521 mm/s in this paper indicate that iron is in Fe^{3+} state. The reason is that it results a distortion in the octahedral with the Sm content increasing and lower the symmetry of the octahedral for the change for B-site. At the same time, the Q.S. values for A-site decrease from 0.62 mm/s to 0.002 mm/s with the Sm content from x=0 to 0.05. With the samariun ions into B-sites instead of the iron ions, it compel the iron ions of B-sites to A-sites. So it has a new distribution in the both A-site and B-site for iron ions. It decreases primary interaction h_{BB}, and makes the hyperfine field diminution. So the hyperfine field of B-site happen a obvious change and the hyperfine field of A-site has a negligible change. In addition, because the magnetic moment of samarium is little than the iron, when the samarium into the sample instead of the iron, it makes the h_{AB} and h_{BA} decease. It knows that the iron ions have a new distribution between the A-site and B-site as the samarium into the Cu-Co ferrite from the Table 1.

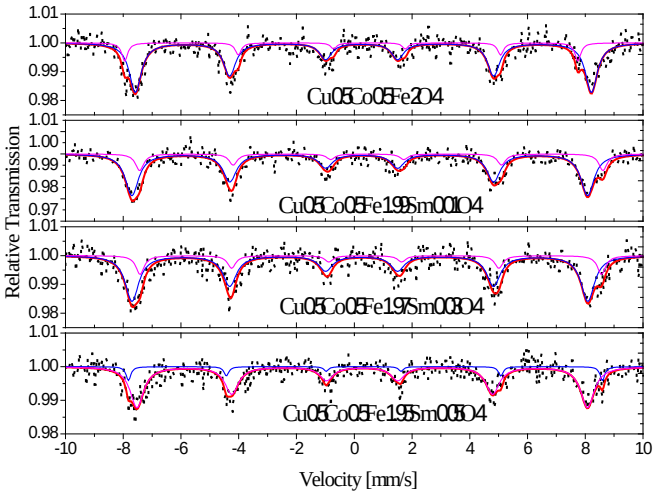

Figure 4: Room temperature Mössbauer spectra of Cu0.5Co0.5Fe2-xSmxO4(x=0~0.05) ferrites.

Table 1: Mössbauer parameters of isomer shift (I.S.), quadrupole splitting (Q.S.), magnetic hyperfine field (H), linewidth (Γ) and absorption area (A0) for Cu0.5Co0.5Fe2-xSmxO4 (x=0~0.05) ferrites calcined at 900 ℃.

Sm	I.S.(mm/s)		Q.S.(mm/s)		H_{hf}(T)		A_0(%)	
content(x)	A	B	A	B	A	B	A	B
0	0.2113	0.2856	-0.6270	0.0608	48.95	50.91	84.7	15.3
0.01	0.2243	0.5212	-0.0672	0.1388	48.93	49.77	80.0	20.0
0.03	0.2256	0.4766	-0.0594	0.1926	48.67	49.57	80.0	20.0
0.05	0.2742	0.3556	0.00207	0.0634	48.38	48.98	89.6	10.4

3.4. Magnetic Property of Particles

Fig.5 shows hysteresis loops of $Cu_{0.5}Co_{0.5}Fe_{2-x}Sm_xO_4$ at room temperature. The magnetization of all samples nearly reaches saturation at the external field of 9000 Oe. It noticed that the samarium into the crystal lattice do not change the ferrimagnetic character of all samples. The ferrimagnetic for the spinel type ferrite depend on the number of atoms of magnetism, magnetic moment of atoms, superexchange interaction and external temperature[11-12].

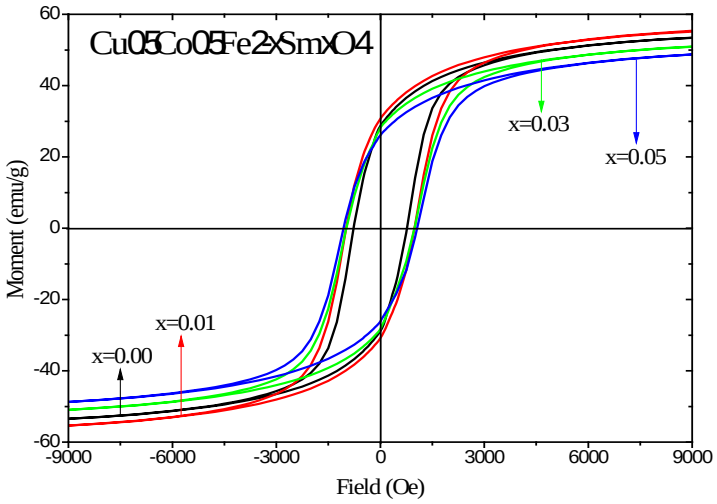

Figure 5: Room temperature hysteresis loops of Cu0.5Co0.5Fe2-xSmxO4 (x=0-0.05).

Table 2: The magnetic parameters of Cu0.5Co0.5Fe2-xSmxO4(x=0-0.05).

Content(x)	M_S (emu/g)	H_C (Oe)	Mr (emu/g)
0.00	53.8976	878.1535	28.6646
0.01	53.6567	878.2367	28.4261
0.03	51.4066	878.1917	28.2060
0.05	49.2636	1128.9615	26.0859

The saturation magnetization first decreases with the different content x of samarium. The follow reasons explain the result: (1)The saturation magnetization could be expressed by means of the following relation[12-14]:

$$\sigma_s = \frac{5585 \times n_B}{M} \tag{2}$$

Where n_B is the magnetic moment with Bohr magneton as the unit, M is relative molecular mass. The relative molecular mass of $Cu_{0.5}Co_{0.5}Fe_{2-x}Sm_xO_4$ increase as Sm content x increases. The change of magnetic moment n_B can be explained with Néel's theory. The magnetic moment of per ion for Sm^{3+}, Cu^{2+}, Co^{2+} and Fe^{3+} ions are 1.5 μ_B, 1.9 μ_B, 3 μ_B and 5 μ_B [15-18], respectively. Because the magnetic moment of samarium is little than the magnetic moment of iron ion. At the

same time, the relative molecular mass of samarium is bigger than the iron. So the saturation magnetism of sample at the room temperature is decreased with the samarium ions instead of the iron ions. (2)With the content x of samarium increase, it makes the iron ions has a new distribution between A-site and B-site. This decreases A-B and B-B superexchange interaction, making the hyperfine field became little. Because the saturation magnetism and the hyperfine field have a relationship[14,19]:

$$M_s = AH_{hf} \tag{3}$$

Where the M_s is the saturation magnetism, H_{hf} is the hyperfine field and the A is the constant. It is noticed that the saturation magnetism decreases with the little hyperfine field from the equation (3). The saturation magnetism becomes being decreased with the little size of particle. The size of particle is discussed in the x ray diffraction and scanning electron microscope.

There is a relationship between the residual magnetization and saturation magnetization[14, 20]:

$$Mr = Ms\overline{\cos\theta} \tag{4}$$

Mr is the residual magnetization, Ms is the saturation magnetization and θ is the angle between the magnetic the magnetic field strength and the easy axis of magnetization. Theoretically, the same change in residual magnetization and saturation magnetization. As can be seen from Table 2, the Mr and Ms have the same diversification. So agreement of theory and experiment is very good.

It is noticed that the coercivity force has a unconspicuous increase when the $x \leq 0.03$. When the $x=0.05$, the coercivity force of the sample abruptly increase up to 1128.9 Oe. The radii of Sm^{3+} ions is larger than that of Fe^{3+} ions, so the symmetry of crystal will be decreased after the sample was substituted by Sm^{3+} ions. It may distort the lattice or crystalline field, and generate an internal stress. Moreover, it is known that the grain boundary increases with decreasing crystallite size. In our study, Sm substituted Cu-Co ferrites have a decrease in crystallite size with the substitution of Sm^{3+} ions[21-23]. The area of disordered arrangement for ions on grain boundaries may fix and hinder the domain walls motion, thus the coercivity of the samples increases with Sm^{3+} ions substituted Cu-Co ferrite. However, when the content $x \leq 0.03$ the coercivity showed no significant changes by increasing the gadolinium content, it may be related to the coercivity is influenced by many factors, such as crystallinity, microstrain, magnetic particle morphology and size distribution, anisotropy and magnetic domain size. When the content $x=0.05$, there is excessive precipitation of Sm^{3+} in the grain boundary form $SmFeO_3$, making the domain wall displacement resistance increase abruptly. This causes coercive force increase quickly.

4. Conclusion

The Cu-Co ferrite particles were prepared by sol-gel method. With the increase of incorporation, the smaller the particle size and the lattice constant decrease. SEM results indicate that particles will be refined, the particle size uniformity is improved with incorporation of Sm^{3+}. Room temperature Mössbauer spectra of $Cu_{0.5}Co_{0.5}Fe_{2-x}Sm_xO_4$ ferrites calcined at 900 ℃ is formed by two normal Zeeman-split sextets. It display ferrimagnetic behavior for the all samples. The incorporation of Sm^{3+} does not affect the outer s electron density of Fe^{3+}. But it will influence the superexchange interactions within the lattice. The results of magnetic measurements show that incorporation of Sm^{3+} makes saturation magnetization and remanence not sigfinicant increases. But the coercivity shows no significant change when the content $x \leq 0.03$, but the coercivity abruptly increase up to 1128.9 Oe when $x=0.05$ with the Sm^{3+} ions doping.

Acknowledgements

This work was financially supported by the National Natural Science Foundation of China (NO.12164006, 11364004) and Guangxi Key Laboratory of Nuclear Physics and Nuclear Technology. Kaimin Su and Guangbai Yuan contributed equally to this work.No potential conflict of interest was reported by the authors.

References

[1] Nikolay Velinov, Kremena Koleva, et al. Nanosized $Cu_{0.5}Co_{0.5}Fe_2O_4$ ferrite as catalyst for methanol decomposition: Effect of preparation procedure. Catalysis Communications 32, (2013): 41-46.

[2] Hongzhe Chen, Shaogui Yang, et al. Efficient degradation of crystal violet in magnetic CuFe2O4 aqueous solution coupled with microwave radiation .Chemosphere, 89 (2012): 185-189.

[3] Ma G, Hao B, Li LC, Chen K, He Y, Qiao R, Li J, Ding Y.Preparation and Electromagnetic Properties of the Co0.6Cu0.16Ni0.24Fe2O4/ Multi-Walled Carbon Nanotube/ Polypyrrole Composites. Science of Advanced Materials, 6 (2014): 298-303.

[4] Ameer Azam. Microwave assisted synthesis and characterization of Co doped Cu ferrite nanoparticles .Journal of Alloys and Compounds, 540 (2012): 145-153.

[5] A.A. Sattar, A.M. Samy. Effect of Sm substitution on the magneticand electrical properties of Cu-Zn ferrite .Journal of Materials Science, 37 (2002): 4499-4502.

[6] Rashad M, Mohamed R, El-Shall h. Magnetic properties of nanocrystalline Sm-substituted CoFe2O4 synthesized by citrate precursor method. Journal of materials processing technology, 2008, 198 (1): 139-146.

[7] Guo L, Shen X, Song F, et al. Structure and magnetic property of CoFe2−xSmxO4 (x=0-0.2) nanofibers prepared by sol-gel route. Materials Chemistry and Physics, 2011, 129 (3): 943-947.

[8] Zhao L, Han Z, Yang H, et al. Magnetic properties of nanocrystalline Ni0.7Mn0.3Gd0.1Fe1.9O4 ferrite at low temperatures. Journal of Magnetism and Magnetic Materials, 2007, 309 (1): 11-14.

[9] Inbanathan S, Vaithyanathan V, Arout Chelvane J, et al. Mössbauer studies and enhanced electrical properties of R (R= Sm, Gd and Dy) doped Ni ferrite. Journal of Magnetism and Magnetic Materials, 2014, 353.41-46.

[10] Kumar S, Farea A, Batoo K M, et al. Mössbauer studies of Co0.5CdxFe2.5−xO4 ($0.0 \leq x \leq 0.5$) ferrite. Physica B: Condensed Matter, 2008, 403 (19): 3604-3607.

[11] S.S. Ata-Allah. XRD and Mossbauer studies of crystallographic and magnetic transformations in synthesized Zn-substituted Cu-Ga-Fe compound .Journal of Solid State Chemistry 177 (2004) 4443-4450.

[12] Gabal, M.A., A.M. Asiri, and Y.M. AlAngari, On the structural and magnetic properties of La-substituted NiCuZn ferrites prepared using egg-white. Ceramics International, 2011. 37(7). 2625-2630.

[13] Al-Hilli M F, Li S, Kassim K S. Structural analysis, magnetic and electrical properties of samarium substituted lithium-nickel mixed ferrites. Journal of Magnetism and Magnetic Materials, 2012, 324 (5): 873-879.

[14] Gadkari A B, Shinde T J, Vasambekar p n. Magnetic properties of rare earth ion (Sm3+) added nanocrystalline Mg-Cd ferrites, prepared by oxalate co-precipitation method. Journal of Magnetism and Magnetic Materials, 2010, 322 (24): 3823-3827.

[15] Liu Y, Zhu X G, Zhang L, et al. Microstructure and magnetic properties of nanocrystalline Co1−xZnxFe2O4 ferrites. Materials research bulletin, 2012, 47 (12): 4174-4180.

[16] Jiang J, Yang Y-m, Li L C. Synthesis and magnetic properties of lanthanum-substituted lithium-nickel ferrites via a soft chemistry route. Physica B: Condensed Matter, 2007, 399 (2): 105-108.

[17] Daengsakul. S, Thomas.C, Mongkolkachit.C, Maensiri.S.Thermal Hydro-Decomposition Synthesis, Structural Characterization, and Magnetic Properties of La1-xSrxMn1-yCoyO3 Nanopowders. Science of Advanced Materials 5 (2013) 242-253.

[18] Zhang, Y. and D. Wen, Infrared emission properties of RE (RE=La, Ce, Pr, Nd, Sm, Eu, Gd, Tb, and Dy) and Mn co-doped Co0.6Zn0.4Fe2O4 ferrites. Materials Chemistry and Physics, 2012. 131(3). 575-580.

[19] Lin J P, Guo Z P, WANG Y L, et al. Mössbauer Spectroscopy and Magnetic Properties of Bi0.8Ca0.2-xSrxFeO3 Nanoparticles by Sol-gel Method. Materials Science, 2019, 25(2): 135-140.

[20] Fang Y, Yang X X, Qing L I N, et al. Microstructure and Magnetic Studies of La1-xSrxFeO3 Nano Particles Fabricated by the Citrate Sol-Gel Method. Materials Science, 2019, 25(3): 231-237.

[21] Nikumbh a, Pawar r, Nighot d, et al. Structural, electrical, magnetic and dielectric properties of rare-earth substituted cobalt ferrites nanoparticles synthesized by the co-precipitation method. Journal of Magnetism and Magnetic Materials, 2014, 355 201-209.

[22] Qing Lin, Qingmei Zhang, Xinlong Dong, Guodong Tang, Yun He, Magnetic and Mössbauer spectra observed for mixed-metal magnets NBu4FeIInMAII1−n [FeIII(OX)3](MA=Mn, Fe) .Hyperfine Interact (2013) 219:77-82 .

[23] Lin Q, Xu J, Yang F, et al. The influence of Ca substitution on LaFeO3 nanoparticles in terms of structural and magnetic properties. Journal of Applied Biomaterials & Functional Materials, 2018, 16(1_suppl): 17-25.